KSÜ Mühendislik Bilimleri Dergisi, 26(Özel Sayı), 2023 KSU J Eng Sci, 26(Special Issue), 2023
9th Uluslararası IFS Çağdaş Matematik ve Mühendislik Konferansı Özel Sayısı
9th International IFS Contemporary Mathematics and Engineering Conference Special Issue
Araştırma Makalesi Research Article

Kahramanmaras Sutcu Imam University
Journal of Engineering Sciences

Geliş Tarihi : 09.08.2023 Received Date : 09.08.2023
Kabul Tarihi : 18.09.2023 Accepted Date : 18.09.2023

EFFECTS OF COMPLETE AND PARTIAL CYLINDRICAL FIN CONFIGURATIONS ON THERMOHYDRAULIC PERFORMANCE OF A MINICHANNEL HEAT SINK

TAM VE PARÇALI SİLİNDİRİK KANATÇIK KONFİGÜRASYONLARININ BİR MİNİKANALLI ISI ALICININ TERMOHİDROLİK PERFORMANSI ÜZERİNDEKİ ETKİLERİ

Buğra SARPER[1*] (ORCID: 0000-0001-7554-6575)
Döndü Nur TÜRK[2] (ORCID: 0009-0004-4144-5361)
Kayhan DAĞIDIR[1] (ORCID: 0000-0003-0499-1764)
Orhan AYDIN[3] (ORCID: 0000-0002-2492-8212)

[1] Tarsus University, Mechanical Engineering Department, Mersin, Turkey
[2] Tarsus University, Outomotive Engineering Department, Mersin, Turkey
[3] Karadeniz Technical University, Mechanical Engineering Department, Trabzon, Turkey

*Sorumlu Yazar / Corresponding Author: Buğra SARPER, bugrasarper@tarsus.edu.tr

ABSTRACT

In this numerical investigation, the impacts of complete and partial cylindrical fin configurations on the thermohydraulic performance of a minichannel heatsink are studied. ANSYS Fluent software is used to conduct numerical analyses for four distinct mass flow rates ranging from 0.00265 kg/s to 0.0045 kg/s and three distinct fin positions. The effects of various configurations on velocity and temperature fields, average Nusselt number, Nusselt number ratio, friction coefficient, and performance evaluation coefficient are analyzed. According to the study's findings, using partial cylindrical fins has a substantial impact on both heat transfer and pressure drop. When evaluating heat transfer, MCHS-R2a produces the greatest results, but this configuration greatly raises flow resistance. MCHS-R2c was found to have substantial potential when evaluated in terms of thermohydraulic performance.

Keywords: Minichannel heat sink, partial cylindrical fin, thermohydraulic performance.

ÖZET

Bu çalışmada, tam ve parçalı silindirik kanatçık konfigürasyonlarının bir minikanallı ısı alıcının termohidrolik performansına etkileri sayısal olarak incelenmiştir. Bu amaçla, 0.00265 kg/s ile 0.0045 kg/s aralığında dört farklı debi ve üç farklı kanatçık konumu için sayısal çalışmalar ANSYS Fluent yazılımı kullanılarak gerçekleştirilmiştir. Farklı konfigürasyonların hız ve sıcaklık alanlarına, ortalama Nusselt sayısına, Nusselt sayısı oranına, sürtünme katsayısına ve ısı alıcının performans katsayısına olan etkileri değerlendirilmiştir. Çalışma sonucunda, parçalı silindirik kanatçık kullanımının ısı transferi ve basınç düşümü üzerinde önemli etkilerinin olduğu, ısı transferi açısından değerlendirildiğinde MCHS-R2a'nın en iyi sonucu verdiği fakat bu konfigürasyonun akışa karşı olan direnci önemli ölçüde artırdığı belirlenmiştir. Termohidrolik performans açısından değerlendirildiğinde ise MCHS-R2c'nin önemli sonuçlar vadettiği ortaya konmuştur.

Anahtar Kelimeler: Minikanallı ısı alıcı, parçalı silindirik kanatçık, termohidrolik performans.

ToCite: SARPER, B., TÜRK, D.N., DAĞIDIR, K. & AYDIN, O., (2023). EFFECTS OF COMPLETE AND PARTIAL CYLINDRICAL FIN CONFIGURATIONS ON THERMOHYDRAULIC PERFORMANCE OF A MINICHANNEL HEAT SINK. *Kahramanmaraş Sütçü İmam Üniversitesi Mühendislik Bilimleri Dergisi*, 26 (Özel Sayı), 1156-1170.

INTRODUCTION

Changing manufacturing techniques and advancing technology have enabled the design and production of compact heat exchangers with reduced volume and greater efficiency. Minichannel heat sinks (MCHSs), a type of compact heat exchangers, have attracted the attention of researchers due to their compact structure, effective thermal performance, and growing application possibilities. As a result of advancements in materials technology, MCHSs have been used as a practical apparatus to remove excessive heat from systems since the mid-1990s (Bowers and Mudawar, 1994). Their prevalence has increased due to their widespread application in electronics cooling.

To meet the ever-increasing demand for cooling, MCHSs have modified to incorporate fins, which contribute to the enhancement of heat transfer characteristics (Naphon and Wongwises, 2010). However, while fins positioned in the flow field increase heat transfer, they negatively affect the pressure drop. This has led to the necessity of addressing the issue in terms of both heat transfer and pressure drop. Researchers have investigated a variety of configurations in channel structure and flow pattern so as to enhance the system's efficiency in terms of both heat transfer and pressure drop. Table 1 provides a summary of various configurations of channel structures and flow patterns reported in the literature.

Table 1. Some Studies on Channel Structures and Flow Patterns in The Literature

Reference	Content of the study
Bi et al. (2013)	The channel with narrow dimples, cylindrical grooves and fins smaller than the channel height.
Wang et al. (2013)	The rectangular straight and expanding cross section of the channel.
Di Maio et al. (2014)	The straight and ribbed channel.
Ghobadi and Muzychka (2014)	The channel with 90° curved and spiral geometry.
Li et al. (2015)	The channel with smooth and grooved surfaces.
Xu et al. (2016)	The channel with three and five ports.
Saeed and Kim. (2016)	The channel with variable fin spacing, thickness and height.
Ma et al. (2016)	The channel with corrugated fins.
Liu and Yu (2016)	The channel with obstacles in the flow direction.
Kim et al. (2017)	The channel with variable widht and length.
Tang (2017)	The channel with layered structure.
Saeed and Kim (2017)	The channel with different configurations of distributors and collectors at the inlet and outlet.
Imran et al. (2018)	The channel with variable inlets and outlets.
Kumar and Singh (2019)	The channel with variable distributor and collector positions.
Abdulhaleem et al. (2019)	The channel with straight and wavy cross sections.
Lim and Lee (2019)	The channel with parallel and opposing flow directions.
Song et al. (2019)	Flow-regulating distributor and collector with trapezoidal and rectangular fins.
Tikadar et al. (2019);	The channel with parallel and opposing flow directions.
Mitra and Ghosh (2020)	The channel with variable fin thickness, number and channel depth.
Xiao et al. (2020)	The channel with rough surface.
Dabrowski (2020)	The channel with rectangular, trapezoidal, triangular or concave configurations.
Cao et al. (2020)	The channel with curved structure with variable inlets and outlets.
Deng et al. (2020)	The channel with horizontal and vertical slots.
Kilic et al. (2020)	The channel with circular fins.
Tikadar (2020);	The channel with transition zones.
Azadi et al. (2020)	The channel containing fins with trapezoidal, square, triangular and sine profiles.

It is clear that the various types of channel structures and flow patterns presented in the literature have an impact on the performance of MCHSs. However, selection of the most effective configuration among many potential configurations is a unique area. Recent studies have examined the effects of both fin and channel forms on heat transfer and pressure drop for optimal heat sink design. Al-Hasani and Freegah (2022) numerically investigated the use of dual outlets and secondary flow lines at various angles to improve the efficiency of a water-cooled MCHS. They reported that combining the secondary flow with pin fins improved thermal and hydraulic performance, and achieved that a performance improvement of up to 47%. Mahmood and Freegah (2022) numerically examined the effect of counterflow formation and dimpled ribs on thermohydraulic performance of a serpentine MCHS. The results

of the study showed that the overall performance of MCHS was significantly improved. Bessanane et al. (2022) numerically investigated the effects of the use of rectangular mini-channels and diamond-shaped fin arrangements in a split pattern on flow and heat transfer in a MCHS. Chen et al. (2022) numerically studied the effects of triangular prisms on thermal and hydraulic performances of a MCHS. The results of the study showed that the highest Nusselt number and coefficient of friction were reached in the MCHS with a backward triangular prism. Khadir (2023) numerically investigated the performance of a finned MCHS with elliptical, circular and V-shaped cross-sections in terms of velocity distribution uniformity and heat sink surface temperature reduction. As a result of the study, it was reported that the lowest flow disturbance and surface temperature were obtained for the channel with elliptical fins. Zhang et al. (2023) numerically investigated the thermohydraulic performance of a MCHS, which contains various mini channel structures with different fin and cavity forms. The results showed that the addition of fins to the mini channel increased heat transfer and flow resistance. In addition, it was stated that the combined use of fin and cavity structures provided 60% improvement in terms of thermohydraulic performance. Accordingly, it is considered that studies on an optimum finned MCHS design in terms of heat transfer and pressure drop will contribute to the literature. The aim of this study is to numerically examine the effects of the use of complete and partial cylindrical fins on thermohydraulic performance of a MCHS. Thus, numerical studies are carried out for the mini channel heat sink designs including reference case (MCHS), complete cylindrical fins (MCHS-R) and partial cylindrical fins (MCHS-R2) under same operating conditions.

NUMERICAL STUDY

Problem Geometry

A schematic illustration of the MCHS containing seven minichannels is shown in Fig. 1. The length (L), width (W), and height (H) of MCHS are 75, 50, and 5 mm, respectively. The minichannels' widths (w_{ch}) and heights (h_{ch}) are 4.2 mm and 2 mm, respectively, and the walls separating them have the thickness (t_w) of 1.77 mm. The distance between the centers of the first and last fins and the channel inlets-outlets is 10 mm. The diameter of each fin is 2 mm, and the distance between each fin (s) is 13.75 mm.

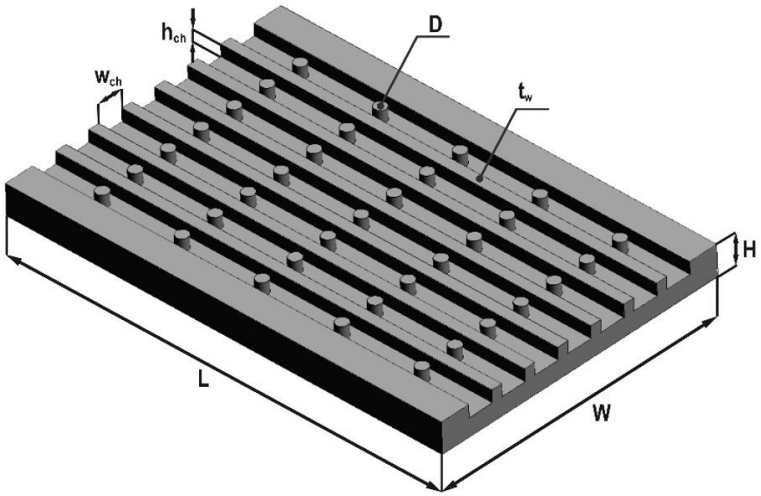

Figure 1. Schematic Illustration of The Minichannel Heat Sink with Complete Cylindrical Fins (MCHS-R)

The study covers five different cases, including the reference case (MCHS). In the reference case, no fin is utilized in the minichannels. In addition, the details of configurations designated MCHS-R, MCHS-R2a, MCHS-R2b, and MCHS-R2c are shown in Fig 2. These different MCHS configurations are analyzed for various flow rates. In MCHS-R2a, the partial fins are concentrically arranged, whereas in MCHS-R2b and MCHS-R2c, the distance between the center of the partial fins is 3.44 mm and 6.88 mm, respectively.

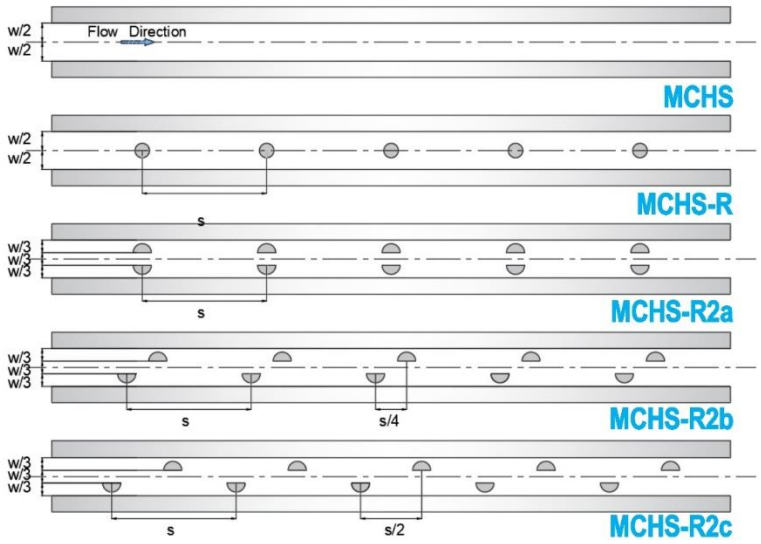

Figure 2. Schematic Illustration of The Studied Cases

Numerical Method and Boundary Conditions

The simulations are conducted using ANSYS Fluent, a finite volume solver. The thermophysical properties of the fluid (water) and heat sink are considered to be constant throughout the numerical solutions, while the flow is at laminar and steady-state conditions. In the numerical solutions, the discretization of the governing equations are performed by the second order upwind scheme, while the SIMPLE algorithm is preferred for the coupling of velocity and pressure (Ansys Inc., 2021).

The governing equations under these assumptions are as follows (Imran et al., 2018):

Continuity equation:

$$\frac{\partial u}{\partial x}+\frac{\partial v}{\partial y}+\frac{\partial w}{\partial z}=0 \tag{1}$$

x-momentum equation:

$$u\frac{\partial u}{\partial x}+v\frac{\partial u}{\partial y}+w\frac{\partial u}{\partial z}=-\frac{1}{\rho}\frac{\partial p}{\partial x}+\vartheta\left(\frac{\partial^2 u}{\partial x^2}+\frac{\partial^2 u}{\partial y^2}+\frac{\partial^2 u}{\partial z^2}\right) \tag{2}$$

y-momentum equation:

$$u\frac{\partial v}{\partial x}+v\frac{\partial v}{\partial y}+w\frac{\partial v}{\partial z}=-\frac{1}{\rho}\frac{\partial p}{\partial y}+\vartheta\left(\frac{\partial^2 v}{\partial x^2}+\frac{\partial^2 v}{\partial y^2}+\frac{\partial^2 v}{\partial z^2}\right) \tag{3}$$

z-momentum equation:

$$u\frac{\partial w}{\partial x}+v\frac{\partial w}{\partial y}+w\frac{\partial w}{\partial z}=-\frac{1}{\rho}\frac{\partial p}{\partial z}+\vartheta\left(\frac{\partial^2 w}{\partial x^2}+\frac{\partial^2 w}{\partial y^2}+\frac{\partial^2 w}{\partial z^2}\right) \tag{4}$$

Energy equation in flow domain:

$$u\frac{\partial T_f}{\partial x}+v\frac{\partial T_f}{\partial y}+w\frac{\partial T_f}{\partial z}=\alpha\left(\frac{\partial^2 T_f}{\partial x^2}+\frac{\partial^2 T_f}{\partial y^2}+\frac{\partial^2 T_f}{\partial z^2}\right) \tag{5}$$

Energy equation in solid domain:

$$\frac{\partial^2 T_s}{\partial x^2} + \frac{\partial^2 T_s}{\partial y^2} + \frac{\partial^2 T_s}{\partial z^2} = 0 \quad (6)$$

Here, u, v, and w represent the velocity components in the x, y, and z directions, while T_f and T_s represent the temperature of the fluid and solid. ρ represents the density of the fluid, while ϑ and α denote its kinematic viscosity and thermal diffusivity.

The velocity inlet boundary condition is employed at the minichannel inlets, and the water temperature is 298 K. The pressure outlet boundary condition is employed at the minichannel outlets. The base of the MCHS is heated with a constant heat flux of 20000 W/m^2, while minichannel and fin surfaces in contact with water have coupled boundary condition and hydrodynamically no-slip boundary condition. The heat sink's top and side faces are perfectly insulated. The boundary conditions are given in Fig. 3.

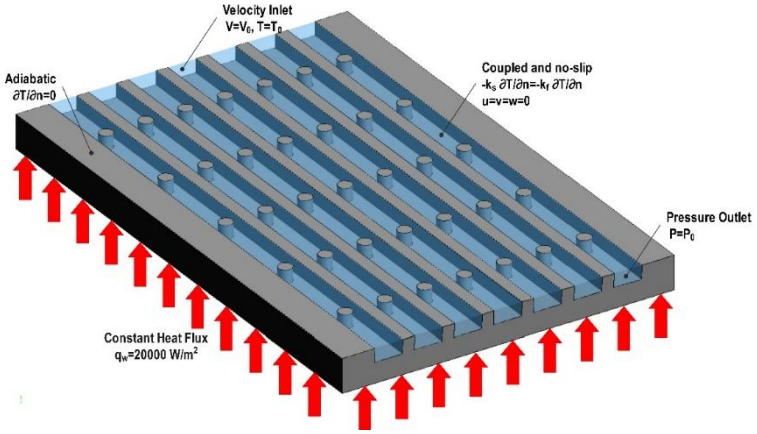

Figure 3. Boundary Conditions Utilized in Numerical Simulations

Data Analysis

As the effects of the above-described configurations on flow and heat transfer characteristics at varying flow rates are evaluated, the following performance parameters are calculated within the scope of the study.

The heat gained by the cooling fluid is calculated as follows (Al-Hasani and Freegah, 2022):

$$\dot{Q} = \dot{m}_f c_{p,f} \Delta T_f = \bar{h} A_c (T_{base,ave} - T_f) \quad (7)$$

where $\dot{m}_f$, $c_{p,f}$, and ΔT_f denote the mass flow rate, specific heat, and temperature rise of water, respectively. A_c denote the effective surface area, while $T_{base,ave}$ and T_f denote the average surface temperature of the base and film temperature, respectively.

The film temperature is calculated as follows:

$$T_f = \frac{T_{f,in} + T_{f,out}}{2} \quad (8)$$

where $T_{f,in}$ and $T_{f,out}$ denote the inlet and outlet temperatures of the water, respectively.

The average heat transfer coefficient is calculated as follows (Imran et al., 2018):

$$\bar{h} = \frac{\dot{m}_f c_{p,f} \Delta T_f}{A_c (T_{base,ave} - T_f)} \quad (9)$$

The average Nusselt number is calculated as follows:

$$Nu_{ave} = \frac{\bar{h}.D_h}{k_f} \tag{10}$$

where k_f is the thermal conductivity of water.

The Nusselt number ratio is calculated as follows:

$$Nu_r = \frac{Nu_{ave,i}}{Nu_{ave,ref}} \tag{11}$$

The hydraulic diameter of the minichannels is calculated as follows:

$$D_h = \frac{2 \times w_{ch} \times h_{ch}}{w_{ch} + h_{ch}} \tag{12}$$

The total pressure drop between the inlet and outlet of the heat sink is calculated as follows:

$$\Delta P = P_{in} - P_{out} \tag{13}$$

The friction coefficient is calculated as follows:

$$f = \frac{2\Delta P D_h}{L\rho_f u_{in}^2} \tag{14}$$

The performance evaluation coefficient, which represents the thermohydraulic performance of the heat sink, is calculated as follows (Zhang et al., 2023):

$$PEC = \frac{Nu_{ort,i}/Nu_{ort,ref}}{(f_i/f_{ref})^{1/3}} \tag{15}$$

where $Nu_{ort,i}$ and $Nu_{ort,ref}$ denote the average Nusselt number for any configuration and reference case, respectively. f_i and f_{ref} denote the friction coefficient for any configuration and reference case, respectively.

Grid Structure

A polyhedral grid design is employed for this research. A grid independence study is conducted for five distinct cell numbers, and the values of average Nusselt numbers and friction coefficients are compared for each grid design to identify the grid design to be employed in the final simulations. When average Nusselt number and friction coefficient are examined simultaneously, as shown in Fig. 4, it is determined that the grid design with 3914104 cells is sufficient for the final simulations.

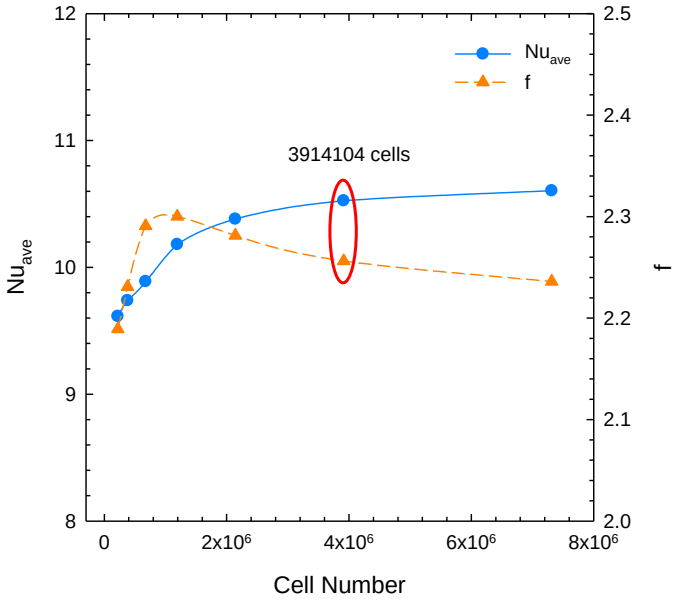

Figure 4. Results of The Grid Independence Study

Validation of the Study

The numerical results of this study are compared to data shared by Al-Hasani and Freegah (2022) for the validation of numerical solution model used in this study. The average Nusselt number and pressure drop characteristics of the MCHS are used for the validation. The relevant data are obtained for different mass flow rates. Accordingly, it is determined that the results of this study is consistent with the data of Al-Hasani and Freegah (2022). Results of the validation study is shown in Fig. 5.

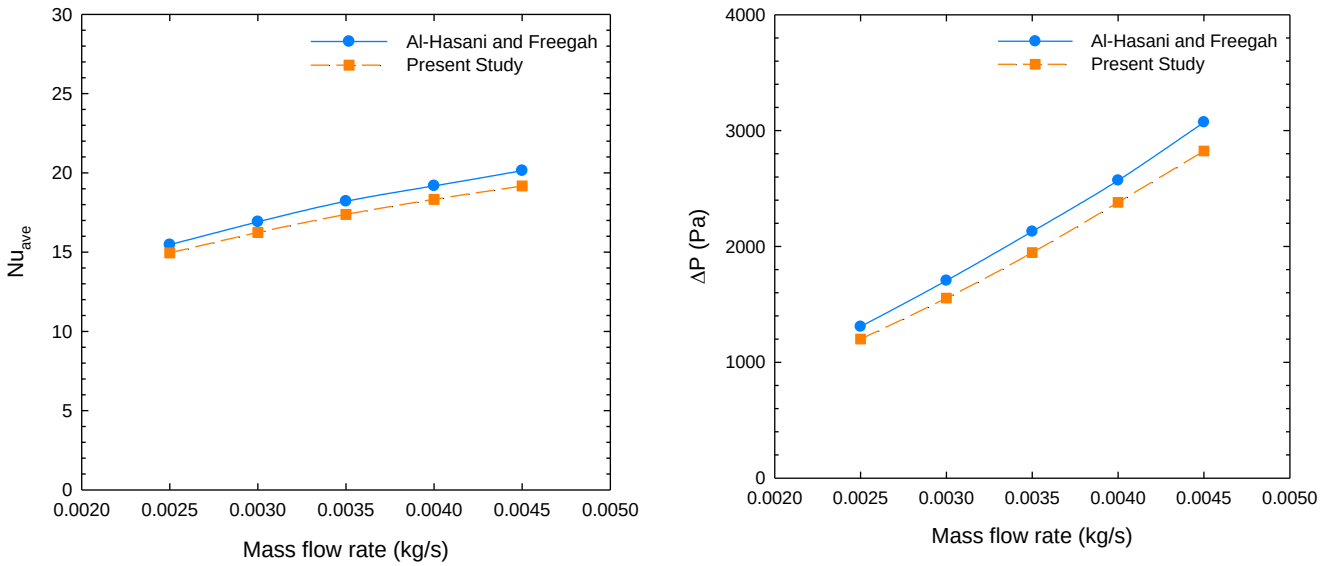

Figure 5. Validation of The Present Study against The Study of Al-Hasani and Freegah (2022)

RESULTS AND DISCUSSION

The impacts of various fin designs on the thermohydraulic performance of a MCHS are numerically studied in this work. The effects of partial and complete cylindrical fins at various flow rates on the flow and heat transfer characteristics of the MCHS are investigated for this purpose. The key performance metrics of the heat sink, such as average Nusselt number, Nusselt number ratio, friction coefficient, and performance evaluation coefficient, are examined in addition to the velocity and temperature fields.

Figures 6 and 7 depict the velocity and temperature fields at the center of the minichannels (at y=4 mm) for various configurations at $\dot{m}_f$=0.002625 kg/s and 0.0045 kg/s, respectively. The flow in MCHS is parallel to the channel walls, as evidenced by the contour plots for both flow rates. In MCHS-R, high velocities occur due to the narrowing of the cross-section in the regions where the fins are placed, while reverse flow occurs downstream of the fins. In MCHS-R2a, the high velocity fluid flows through the partial fins. In MCHS-R2b and MCHS-R2c, the mixing within the flow domain is higher, while local velocities are lower behind the fins and along the channel walls. When the temperature contours are analyzed, the thermal boundary layer thickens towards the exit due to the decreased cooling capacity of the fluid, convective heat transfer diminishes, and the local temperatures of the heat sink increase in MCHS. The addition of fins, on the other hand, increases the heat transfer surface area, allowing the water to remove more heat from the heat sink. The partial fin form also allows for more heat transfer surface area. As a result, the fin temperatures rise towards the outlet, and in all configurations, the temperatures of the fins and fluid are relatively close towards the outlet.

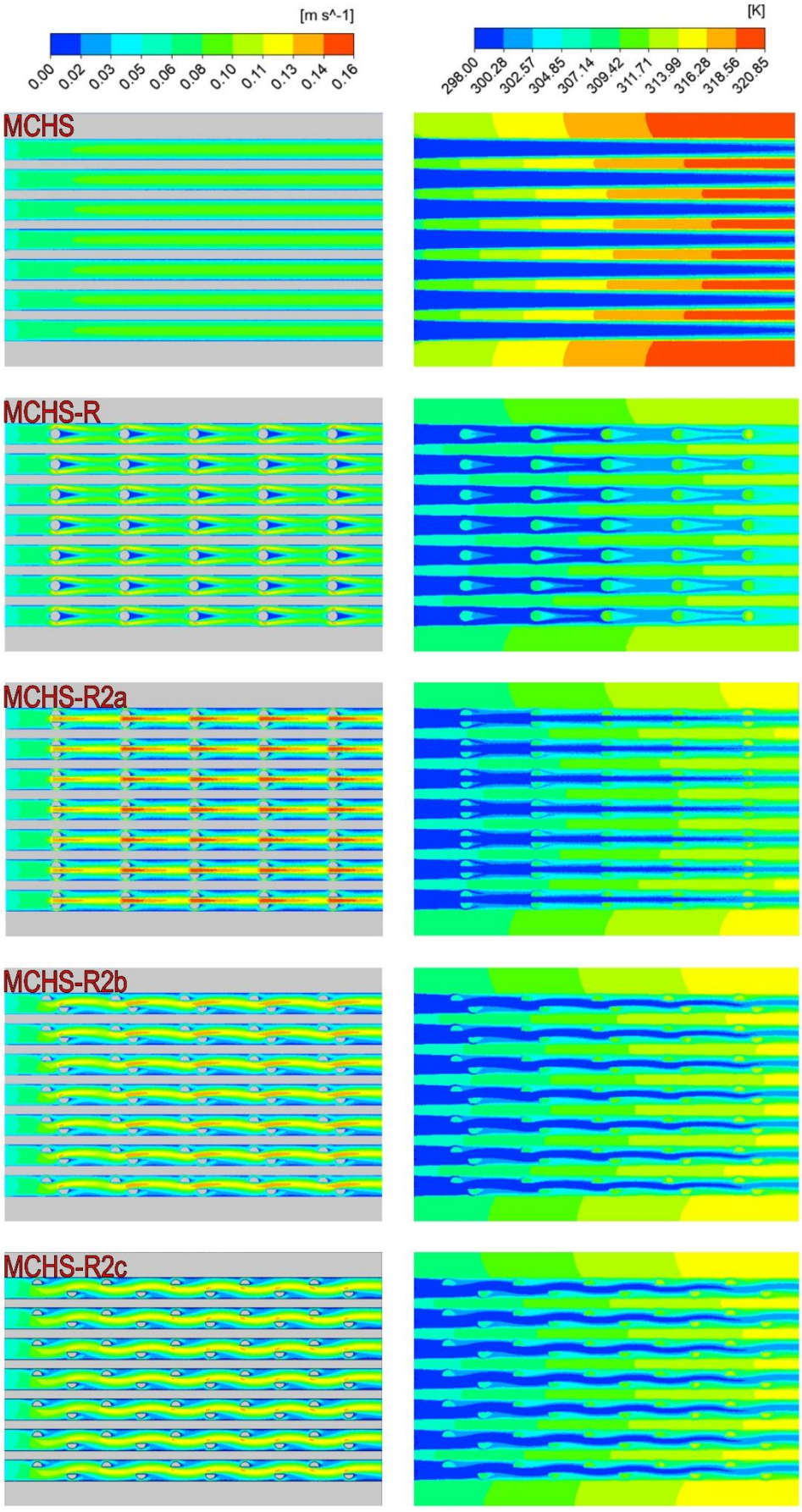

Figure 6. Velocity and Temperature Fields at $\dot{m}_f$=0.002625 kg/s

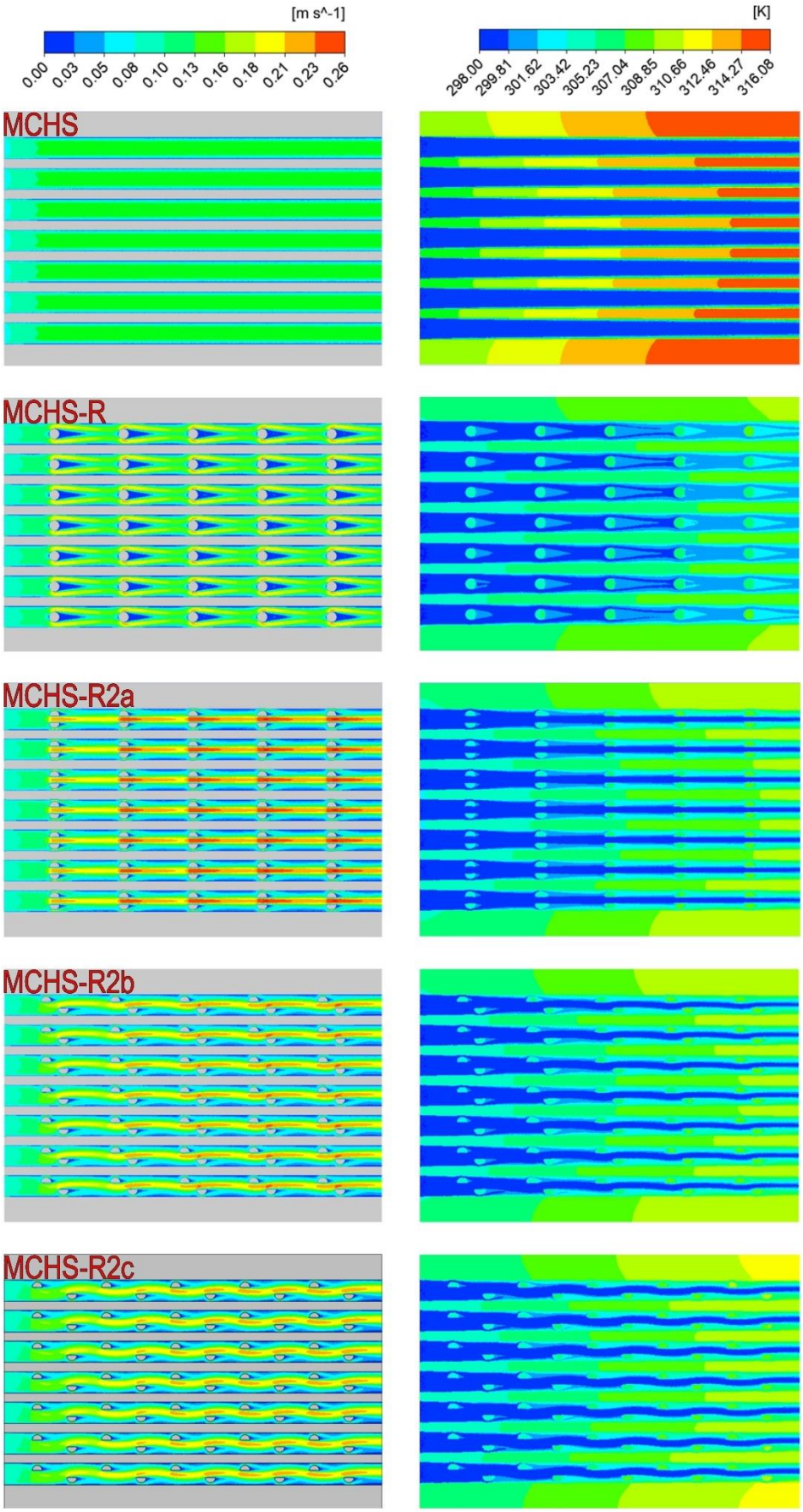

Figure 7. Velocity and Temperature Fields at $\dot{m}_f$=0.0045 kg/s

Figures 8 and 9 depict the Nu_{ave} and Nu_r variations with mass flow rate for the reference case and various fin configurations. Convective heat transfer is the weakest in the reference case, as predicted. In terms of convective heat transfer, however, MCHS-R2a is seen to be the best configuration. At all flow rates, the convective heat transfer rates for MCHS-R2b and MCHS-R2c are quite close to each other. However, the Nu_{ave} for MCHS-R2c is lower than that of the MCHS-R2a. The variation of Nu_r, as shown in Fig. 9, also confirms the preceding conclusions. At all flow rates, the increase in Nu_r is maximum for MCHS-R2a. Nu_r values are close for MCHS-R2b and MCHS-R2c and the increase in MCHS-R2c becomes more apparent as the flow rate increases. Furhermore, MCHS-R is regarded the worst scenario in terms of Nu_r increase and is nearly unaffected by the change in mass flow rate.

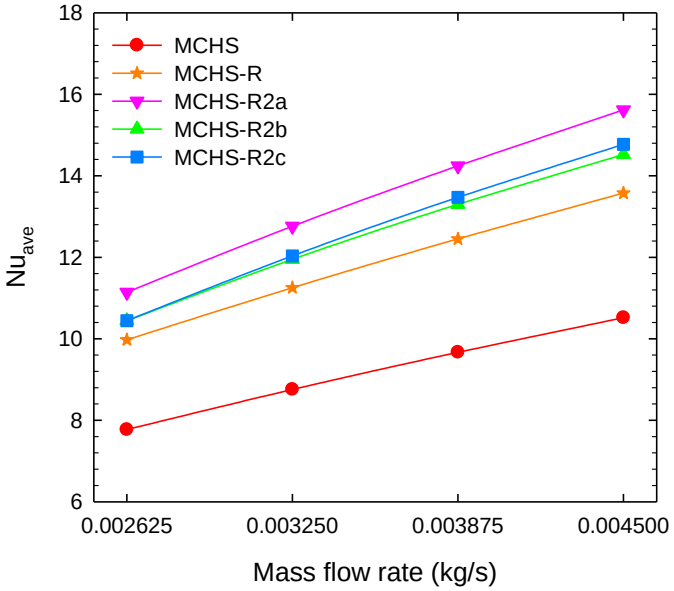

Figure 8. Average Nusselt Number Variation Versus Mass Flow Rate for Different Configurations

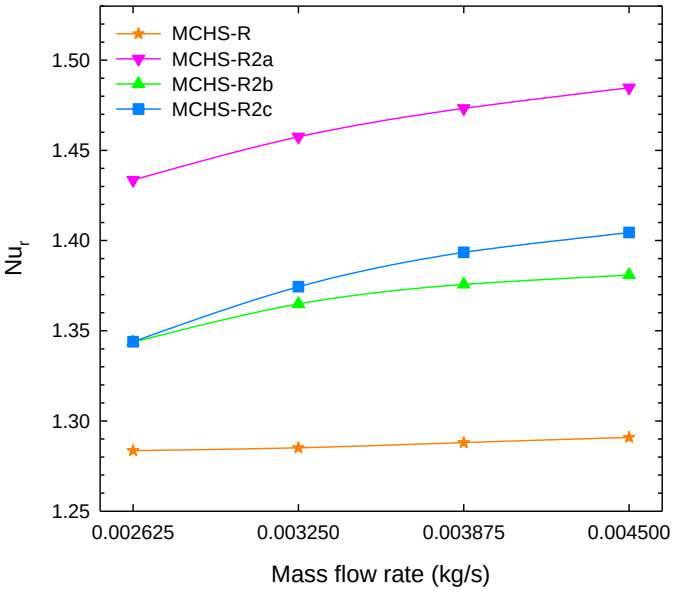

Figure 9. Nusselt Number Ratio Variation Versus Mass Flow Rate for Different Configurations

Figure 10 depicts the relationship between the f and mass flow rate for various fin configurations and the reference case. As anticipated, the f for the reference case (MCHS) is quite low, whereas the utilization of fins considerably increases the f. MCHS-R2a has the greatest flow resistance. MCHS-R2b and MCHS-R2c, whose fins are staggered, have a lower f than that of MCHS-R and MCHS-R2a at all flow rates. When fin configurations are evaluated, increasing the distance between the partial fins substantially decreases the f, and MCHS-R2c has the lowest f values. On the other hand, Fig. 11 illustrates the effects of various fin configurations on the PEC. Analyzing the variation of

PEC with mass flow rate reveals that the thermohydraulic performance of MCHS-R is unfavorable at low mass flow rates, but slightly exceeds 1 as the flow rate increases. MCHS-R2a provides the highest f. Although MCHS-R2c does not provide the greatest convective heat transfer rate, its thermohydraulic performance is significantly higher than the other configurations due to its reduced flow resistance.

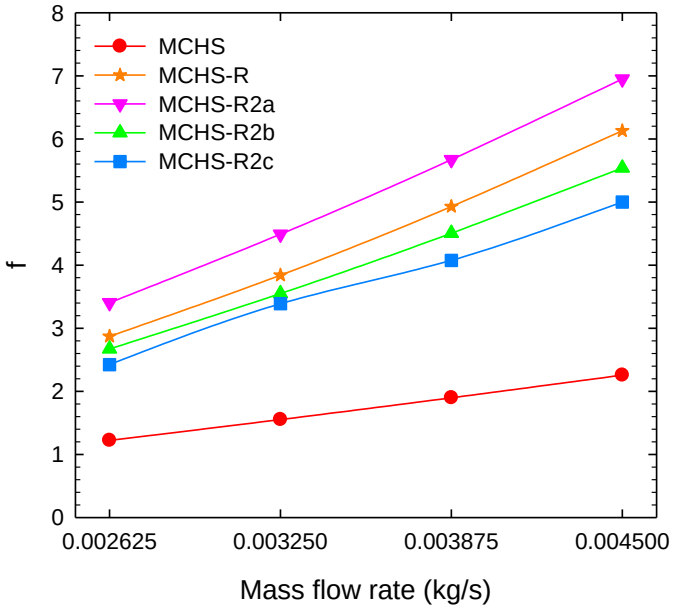

Figure 10. Friction Coefficient Variation Versus Mass Flow Rate for Different Configurations

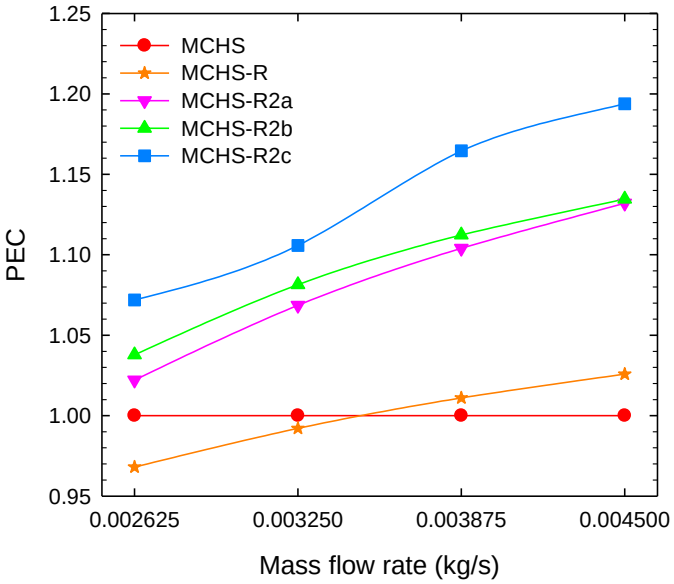

Figure 11. Performance Evaluation Coefficient Variation Versus Mass Flow Rate for Different Configurations

CONCLUSIONS

In this study, the effects of using complete and partial cylindrical fins on thermohydraulic performance of a MCHS are numerically investigated. Additionally, three different partial circular fin forms are proposed as an alternative to the use of traditional cylindrical fins. As a result, the detected findings are as follows:

- It is ensured that the water removes more heat from the heat sink as the heat transfer surface area increases owing to the use of fins. At the same time, the partial fin form further increases the heat transfer surface area.
- It is obtained that the best design in terms of convective heat transfer is the MCHS-R2a configuration. Additionally, MCHS-R2a has the greatest flow resistance.
- It is seen that the use of eccentric partial fins significantly reduces the flow resistance.

- It is observed that the MCHS-R2c configuration provides the best result in terms of thermohydraulic performance. Compared to MCHS, PEC is increased up to 19.4% in MCHS-R2c.

REFERENCES

Abdulhaleem, A. A., Jaffal, H. M., & Khudhur, D. S. (2019). Performance optimiation of a cylindrical mini-channel heat sink using hybrid straight-wavy channel. *International Journal of Thermal Sciences*, *146*, 106111. https://doi.org/10.1016/j.ijthermalsci.2019.106111

Al-Hasani, H. M., & Freegah, B. (2022). Influence of secondary flow angle and pin fin on hydro-thermal evaluation of double outlet serpentine mini-channel heat sink. *Results in Engineering*, *16*, 100670. https://doi.org/10.1016/j.rineng.2022.100670

Ansys Inc. (2021). ANSYS Fluent, Release 21 R2, Theory Guide.

Azadi, M., Hosseinirad, E., Hormozi, F., & Rashidi, S. (2020). Second law analysis for nanofluid flow in mini-channel heat sink with finned surface: a study on fin geometries. *Journal of Thermal Analysis and Calorimetry*, *140*(4), 1883-1895. https://doi.org/10.1007/s10973-019-08921-2

Bessanane, N., Si-Ameur, M., & Rebay, M. (2022). Numerical Study of the Temperature Effects on Heat Transfer Coefficient in Mini-Channel Pin-Fin Heat Sink. *International Journal of Heat and Technology*, *40*(1), 247-257. https://doi.org/10.18280/ijht.400129

Bi, C., Tang, G. H., & Tao, W. Q. (2013). Heat transfer enhancement in mini-channel heat sinks with dimples and cylindrical grooves. *Applied Thermal Engineering*, *55*(1-2), 121-132. https://doi.org/10.1016/j.applthermaleng.2013.03.007

Bowers, M. B., & Mudawar, I. (1994). High flux boiling in low flow rate, low pressure drop mini-channel and micro-channel heat sinks. *International Journal of Heat and Mass Transfer*, *37*(2), 321-332. https://doi.org/10.1016/0017-9310(94)90103-1

Cao, X., Liu, H., Shao, X., Shen, H., & Xie, G. (2020). Thermal performance of double serpentine minichannel heat sinks: Effects of inlet-outlet arrangements and through-holes. *International Journal of Heat and Mass Transfer*, *153*, 119575. https://doi.org/10.1016/j.ijheatmasstransfer.2020.119575

Chen, Z., Feng, Z. F., Zhang, Q. Y., Zhang, J. X. & Guo, F. W. (2022). Effects of regular triangular prisms on thermal and hydraulic characteristics in a minichannel heat sink, *Internatıonal Journal of Heat And Mass Transfer*, *188*. https://doi.org/10.1016/j.ijheatmasstransfer.2022.122583.

Dabrowski, P. (2020). Thermohydraulic maldistribution reduction in mini heat exchangers, *Applıed Thermal Engıneerıng*, *173*. https://doi.org/10.1016/j.applthermaleng.2020.115271.

Deng, Z. Y., Shen, J., Dai, W., Liu, Y., Song, Q., Gong, W., Li, K., & Gong, M. (2020). Flow and thermal analysis of hybrid mini-channel and slot jet array heat sink. *Applied Thermal Engineering*, *171*, 115063. https://doi.org/10.1016/j.applthermaleng.2020.115063

Di Maio, E., Mastrullo, R., Mauro, A. W., & Toto, D. (2014). Thermal management of a multiple mini-channel heat sink by the integration of a thermal responsive shape memory material. *Applied Thermal Engineering*, *62*(1), 113-122. https://doi.org/10.1016/j.applthermaleng.2013.08.039

Ghobadi, M., & Muzychka, Y. S. (2014). Heat transfer and pressure drop in mini channel heat sinks. *Heat Transfer Engineering*, *36*(10), 902-911. https://doi.org/10.1080/01457632.2015.965097

Imran, A. A., Mahmoud, N. S., & Jaffal, H. M. (2018). Numerical and experimental investigation of heat transfer in liquid cooling serpentine mini-channel heat sink with different new configuration models. *Thermal Science and Engineering Progress*, *6*, 128-139. https://doi.org/10.1016/j.tsep.2018.03.011

Khdair, A. I. (2023). Numerical simulation of heat transfer of two-phase flow in mini-channel heat sink and investigation the effect of pin-fin shape on flow maldistribution. *Engineering Analysis with Boundary Elements*, *150*, 385-393. https://doi.org/10.1016/j.enganabound.2023.02.017

Kilic, M., Aktas, M., Sevilgen, G., (2020). Thermal assessment of laminar flow liquid cooling blocks for led circuit boards used in automotive headlight assemblies. *Energies*, *13*(5), 1202-1202. https://doi.org/10.3390/en13051202

Kim, Y., Kim, M., Ahn, C., Kim, H. U., Kang, S. W., & Kim, T. (2017). Numerical study on heat transfer and pressure drop in laminar-flow multistage mini-channel heat sink. *International Journal of Heat and Mass Transfer*, *108*, 1197-1206. https://doi.org/10.1016/j.ijheatmasstransfer.2016.12.025

Kumar, S., & Singh, P. K. (2019). Effects of flow inlet angle on flow maldistribution and thermal performance of water cooled mini-channel heat sink. *International Journal of Thermal Sciences*, *138*, 504-511. https://doi.org/10.1016/j.ijthermalsci.2019.01.014

Li, R. R., Zhang, Y. H., Wang, Y. F., & Wang, L. B. (2015). Convective heat-transfer characteristics of a channel with one surface having mini-grooves in the flow direction and a plain surface located at a mini-distance. *IEEE Transactions on Components, Packaging and Manufacturing Technology*, *5*(1), 65-74. https://doi.org/10.1109/tcpmt.2014.2373054

Lim, K., & Lee, J. (2019). 1-D two-phase flow analysis for interlocking double layer counter flow mini channel heat sink. *International Journal of Heat and Mass Transfer*, *135*, 305-317. https://doi.org/10.1016/j.ijheatmasstransfer.2019.01.092

Liu, X. Q., & Yu, J. (2016). Numerical study on performances of mini-channel heat sinks with non-uniform inlets. *Applied Thermal Engineering*, *93*, 856-864. https://doi.org/10.1016/j.applthermaleng.2015.09.032

Ma, L., Zhao, X., Sun, H., Wu, Q., & Liu, W. (2016). Experimental study of single phase flow in a closed-loop cooling system with ıntegrated mini-channel heat sink. *Entropy*, *18*(6), 128. https://doi.org/10.3390/e18060128

Mahmood, H., & Freegah, B. (2022). Investigating the effect of counter flow formation, ribs and dimples on the hydrothermal performance of the serpentine Mini-Channel Heat Sink (SMCHS). *International Communications in Heat and Mass Transfer*, *139*, 106490. https://doi.org/10.1016/j.icheatmasstransfer.2022.106490

Mitra, I., & Ghosh, I. (2020). Mini-channel heat sink parameter sensitivity based on precise heat flux re-distribution. *Thermal Science and Engineering Progress*, *20*, 100717. https://doi.org/10.1016/j.tsep.2020.100717

Naphon, P., & Wongwises, S. (2010). Investigation on the jet liquid impingement heat transfer for the central processing unit of personal computers. *International Communications in Heat and Mass Transfer*, *37*(7), 822-826. https://doi.org/10.1016/j.icheatmasstransfer.2010.05.004

Saeed, M., & Kim, M. H. (2016). Numerical study on thermal hydraulic performance of water cooled mini-channel heat sinks. *International Journal of Refrigeration*, *69*, 147-164. https://doi.org/10.1016/j.ijrefrig.2016.05.004

Saeed, M., & Kim, M. H. (2017). Header design approaches for mini-channel heatsinks using analytical and numerical methods. *Applied Thermal Engineering*, *110*, 1500-1510. https://doi.org/10.1016/j.applthermaleng.2016.09.069

Song, J. Y., Hah, S., Kim, D., & Kim, S. M. (2019). Enhanced flow uniformity in parallel mini-channels with pin-finned inlet header, *Applied Thermal Engineering*, *152*, 718-733. https://doi.org/10.1016/j.applthermaleng.2019.02.069

Tang, B., Zhou, R., Bai, P., Fu, T., Lu, L., & Zhou, G. (2017). Heat transfer performance of a novel double-layer mini-channel heat sink. *Heat and Mass Transfer*, *53*(3), 929-936. https://doi.org/10.1007/s00231-016-1869-3

Tikadar A., Paul, T. C., Oudah, S. K., Abdulrazzaq, N. M., Salman, A. S., & Khan, J. A. (2020). Enhancing thermal-hydraulic performance of counter flow mini-channel heat sinks utilizing secondary flow: Numerical study with experimental validation. *International Communications in Heat and Mass Transfer*, *111*, 104447. https://doi.org/10.1016/j.icheatmasstransfer.2019.10444

Tikadar, A., Oudah, S. K., Paul, T. C., Salman, A. S., Morshed, A. K. M. M., & Khan, J. A. (2019). Parametric study on thermal and hydraulic characteristics of inter-connected parallel and counter flow mini-channel heat sink. *Applied Thermal Engineering*, *153*, 15-28. https://doi.org/10.1016/j.applthermaleng.2019.02.007

Wang, H. L., Wu, H. C., Wang, S. K., Hung, T. C., & Yang, R. J. (2013). A study of mini-channel thermal module design for achieving high stability and high capability in electronic cooling. *Applied Thermal Engineering*, *51*(1-2), 1144-1153. https://doi.org/10.1016/j.applthermaleng.2012.10.007

Xiao, H., Liu, Z., & Liu, W. (2020). Turbulent heat transfer enhancement in the mini-channel by enhancing the original flow pattern with v-ribs. *International Journal of Heat and Mass Transfer*, *163*, 120378. https://doi.org/10.1016/j.ijheatmasstransfer.2020.120378

Xu, S., Yang, L., Li, Y., Wu, Y., & Hu, X. (2016). Experimental and numerical investigation of heat transfer for two-layered microchannel heat sink with non-uniform heat flux conditions. *Heat and Mass Transfer*, *52*(9), 1755-1763. https://doi.org/10.1007/s00231-015-1691-3

Zhang, Q. Y., Li, Z. Z., Feng, Z. F, Chen, Z., Zhang, J. X. & Guo, F. W. (2023). Effects of combination modes of different cavities and ribs on performance in mini-channels - A comprehensive study. *International Communications in Heat and Mass Transfer*, *142*, 106633. https://doi.org/10.1016/j.icheatmasstransfer.2023.106633